Cerebral Cortex, September 2017;27: 4478–4491

doi: 10.1093/cercor/bhw250
Advance Access Publication Date: 1 September 2016
Original Article

ORIGINAL ARTICLE

Impaired Frontal-Limbic White Matter Maturation in Children at Risk for Major Depression

Yuwen Hung[1], Zeynep M. Saygin[1], Joseph Biederman[2,3], Dina Hirshfeld-Becker[2], Mai Uchida[2,3], Oliver Doehrmann[1], Michelle Han[1], Xiaoqian J. Chai[1], Tara Kenworthy[3], Pavel Yarmak[4], Schuyler L. Gaillard[5], Susan Whitfield-Gabrieli[1], and John D. E. Gabrieli[1,2,5,6]

[1]McGovern Institute for Brain Research, Massachusetts Institute of Technology, Cambridge, MA 02139, USA, [2]Department of Psychiatry, Harvard Medical School, Boston, MA 02115, USA, [3]Clinical and Research Program in Pediatric Psychopharmacology, Massachusetts General Hospital, Boston, MA 02114, USA, [4]Psychology and Neuroscience, University of Toronto, Toronto, Canada, ON M5S 1A1, [5]Department of Brain and Cognitive Sciences, MIT, Cambridge, MA 02139, USA, and [6]Institute for Medical Engineering and Science, MIT, Cambridge, MA 02139, USA

Address correspondence to Yuwen Hung, McGovern Institute for Brain Research, Massachusetts Institute of Technology, 43 Vassar St, 46–5081, Building 46, Cambridge, MA 02139, USA. Email: yuwenh@mit.edu

Abstract

Depression is among the most common neuropsychiatric disorders. It remains unclear whether brain abnormalities associated with depression reflect the pathological state of the disease or neurobiological traits predisposing individuals to depression. Parental history of depression is a risk factor that more than triples the risk of depression. We compared white matter (WM) microstructure cross-sectionally in 40 children ages 8–14 with versus without parental history of depression (At-Risk vs. Control). There were significant differences in age-related changes of fractional anisotropy (FA) between the groups, localized in the anterior fronto-limbic WM pathways, including the anterior cingulum and the genu of the corpus callosum. Control children exhibited typical increasing FA with age, whereas At-Risk children exhibited atypical decreasing FA with age in these fronto-limbic regions. Furthermore, dorsal cingulate FA significantly correlated with depressive symptoms for At-Risk children. The results suggest maturational WM microstructure differences in mood-regulatory neurocircuitry that may contribute to neurodevelopmental risk for depression. The study provides new insights into neurodevelopmental susceptibility to depression and related disabilities that may promote early preventive intervention approaches.

Key words: anterior cingulate, diffusion tensor imaging, frontal–limbic connectivity, major depression

Major depressive disorder (MDD) is one of the most common neuropsychiatric disorders, with the peak ages of diagnosis from adolescence to early adulthood (Lewinsohn et al. 1994; Weissman et al. 2006). Although neuroimaging studies have identified functional and structural brain alterations in adult MDD (Sacher et al. 2012), it remains unclear whether these differences reflect the pathological state of depression itself, or indicate neurobiological traits that predispose individuals to be at risk for depression. Here, we sought to identify neurodevelopmental markers related to increased risk for depression by measuring brain structure differences in children and young teenagers (ages 8–14) who were at enhanced risk for depression

by virtue of having a parent with a history of MDD, which increases the risk of MDD by 3.2 times (Williamson et al. 2004). We employed diffusion weighted imaging (DWI) and assessed white matter (WM) microstructural differences in unaffected children with versus without familial risk for depression. Longitudinal research finds that children with at least 1 depressed parent have about a 3-fold greater risk for developing affective disorders between ages 15 and 30 (Weissman et al. 2006). The goal of this study was to identify neuroanatomical risk markers of depression in children that could help to better understand the developmental predisposition for MDD and contribute toward preventive and early intervention approaches to reduce the risk for MDD.

Previous DWI research on adults and youth with MDD has frequently reported WM abnormalities, primarily lower fractional anisotropy (FA), in limbic and related frontal tracts such as the uncinate fasciculus and the cingulum (Drevets et al. 2008; Zhang et al. 2012; de Kwaasteniet et al. 2013; LeWinn et al. 2014). The locations and connectivity of the altered WM tracts are consistent with evidence that frontal and limbic regions connected by these tracts, such as the anterior/subgenual cingulate (Drevets et al. 1997; Ongur et al. 1998) and amygdala (Stuhrmann et al. 2011), are often affected in MDD. Furthermore, alterations of microstructural properties in anterior cingulate-limbic WM have been predictive of antidepressant treatment outcome in depressed adults (Korgaonkar et al. 2014). However, DWI findings on WM microstructure in youths with MDD are more mixed than that in adults with MDD, perhaps reflecting dynamic brain changes that occur during development. For example, one study reported that adolescents with MDD showed lower FA in bilateral uncinate fasciculi (LeWinn et al. 2014), whereas another study reported higher FA in the uncinate fasciculus (Aghajani et al. 2014) (age ranges in both studies were between 13 and 18 years).

Family history of depression has been found to be associated with brain differences in healthy youths who do not have, or do not yet have, depression. Neuroimaging studies revealed differences in amygdala-cingulate-prefrontal circuitry associated with emotion and emotion regulation between children with versus without familial risk for depression, as measured by functional magnetic resonance imaging (fMRI) task activation (Monk et al. 2008; Mannie et al. 2011; Chai et al. 2015b), functional connectivity during resting state (Luking et al. 2011; Chai et al. 2015a), and amygdala volume (Chai et al. 2015b). Furthermore, a study of cortical thickness in adolescent daughters of mothers with recurrent depression found impaired development in cortical thickness in the anterior cingulate that was associated with the ability to manage sadness (Foland-Ross et al. 2015). Only one study has compared WM microstructure between unaffected adolescents and young adults (12–20 years old) who did or did not have a parent with MDD, and it reported a general reduction in FA in those with parental MDD, involving multiple WM tracts including the uncinate, cingulum, corpus callosum, bilateral superior longitudinal fasciculi, and bilateral inferior fronto-occipital fasciculi (Huang et al. 2011).

In this study, we compared WM microstructure between children with versus without familial (parental) depression in a design that differed in 2 main ways from prior studies. First, we examined WM in a younger age group (from ages 8 to 14), before any onset of syndromatic depression. Second, we aimed to identify specific WM differences between groups that were modulated by brain development across age. Because WM undergoes significant changes during development and neuromaturational rates vary at different developmental periods (Lebel et al. 2012), age may play a crucial role in how neurodevelopment impacts risk for neuropsychiatric disorders. We hypothesized that 1) at-risk children with familial depression may show altered neurodevelopment in the WM that connects brain regions known to be functionally or structurally altered in MDD (Monk et al. 2008; Huang et al. 2011; Luking et al. 2011; Mannie et al. 2011; Chai et al. 2015a, 2015b; Foland-Ross et al. 2015), and 2) that this difference in WM could change with age in the at-risk versus the control children as the at-risk children approach the adolescent ages when affective disorders are most likely to begin to manifest (Lewinsohn et al. 1994; Weissman et al. 2006).

The most widely examined measure of WM microstructure is FA, which typically increases in healthy children from childhood and adolescence to young adulthood in the majority of WM tracts (Giorgio et al. 2008; Lebel et al. 2012; Mwangi et al. 2013). Here, we implemented advancements in DWI analysis by using TBSS (Track-Based Spatial Statistics) (Smith et al. 2004, 2006) and TRACULA (TRActs Constrained by UnderLying Anatomy) (Yendiki et al. 2011). First, whole-brain assessment was implemented using TBSS in order to identify local WM regions that showed significant differences between groups or significant developmental differences between groups (interaction of age × group). Second, any region of interest (ROI) that showed a significant FA difference was further characterized by examinations of radial diffusivity (RD), axial diffusivity (AD), and mean diffusivity (MD) measures. Third, connectivity pathways associated with that ROI were examined by TRACULA tract-based assessments.

Materials and Methods

Participants

Twenty offspring (ages 8–14) of parents with lifetime history of MDD (At-Risk group; mean age 11.1 ± 1.57 years) and 20 age-matched offspring of parents with no lifetime MDD (Control group; mean age 10.65 ± 2.12 years) participated in this study. Eligible participants recruited for the study were right-handed, had normal or corrected-to-normal visual acuity, had a working command of the English language, and IQ scores higher than 85 (one standard deviation (SD) from the average). Exclusion criteria included the presence of acute psychosis or suicidal ideations in parents or the child; lifetime history of bipolar disorder in the parent, lifetime depression or autism in the child, or a history of traumatic brain injury or neurological disorder in the child. Children who had conditions incompatible with undergoing magnetic resonance imaging (MRI), such as claustrophobia, metal implants, braces, electronically, mechanically, or magnetically activated devices such as cochlear implants, were also excluded from the study. The participants in this study overlap with those who participated in 2 prior fMRI studies (Chai et al. 2015a, 2015b). The participants in this study were those who had high-quality DWI scans for this study. Detailed participant recruitment processes can be seen in the Supplementary material.

This study was approved by the Institutional Review Board at the Massachusetts General Hospital and the Institutional Review Board at the Massachusetts Institute of Technology. Before participation, parents provided written informed consent for their child to participate the study, and all youths provided written assent.

Diagnostic Interview

Each child and both their parents were assessed for current and lifetime mood disorders (major depression, bipolar disorder, and dysthymia) using structured clinical interviews in which the mother was the informant at the time of enrollment for this study. For the parental interview, we used the depression, mania, dysthymia, and psychosis modules from the SCID (First et al. 1995). For the child interview, we used the depression, mania, dysthymia, and psychosis modules from the Schedule of Affective Disorders and Schizophrenia for School-Aged Children–Epidemiological Version (KSADS-E) for Diagnostic and Statistical Manual of Mental Disorders, Fourth Edition (DSM-IV) (Orvaschel 1994).

Clinical Behavioral Assessments

General Cognitive Function (IQ)

General cognitive functioning was assessed using the Kaufman Brief Intelligence Test-2 (KBIT-2), a 20-min screening for verbal and nonverbal cognitive performances (Kaufman and Kaufman 2004).

Behavioral Problems

We asked mothers to complete the Child Behavior Checklist (CBCL) (Achenbach and Rescorla 2001) about their child to assess current behavioral and emotional problems of the children. The CBCL also includes subscales reflecting internalizing symptoms (affective and anxiety) and externalizing (attentional and disruptive behavioral) problems. None of the children included in this study had CBCL scores falling in the clinical range (standard scores were below 70).

Depressive Symptoms

The Child Depression Inventory (CDI) (Kovacs 1985) was administered to all children by self-report, which assessed current depressive symptoms (total score) and included 5 factors: negative mood, interpersonal problems, ineffectiveness, anhedonia, and negative self-esteem.

Participant Demographics

Children in the At-Risk and Control groups did not differ significantly in age, IQ, or gender distribution (independent-samples *t*-tests). The At-Risk group had significantly higher scores than the Control group on the CBCL total score [$t(38) = 2.24$, $P < 0.05$; independent-samples *t*-test]; none of the CBCL subscales differed significantly between groups (Table 1). All participants' CBCL scores were below the clinical cutoff point (<70). The 2 groups did not differ significantly in total CDI scores (Table 1). Detailed information regarding clinical behavioral assessment is reported in the Supplementary material.

Imaging Procedure

MRI data were collected at MIT using a Siemens 3 T Magnetom Tim Trio scanner (Siemens, Erlangen, Germany) with a 32-channel head coil. Diffusion-weighted images were collected in the same scan session as the T1-weighted whole-head anatomical images (MPRAGE sequence, 1×1.2 mm in-plane resolution, 1.2 mm slice thickness, field of view (FOV) = 210 mm, matrix = 210×210, 176 slices, TE = 1.64 ms, maximum TE = 7.1 ms, TR = 2.53 s). Diffusion-weighted series included 10 nondiffusion weighted reference volumes (b = 0) and 30 diffusion-weighted volumes (b = 700 s/mm2). The acquisition parameters were as follows: in-plane resolution = 2.0 mm isotropic, matrix size = 128×128, FOV = 256 mm chosen for full-brain coverage, TE = 84 ms, and TR = 8.04 s.

Data Processing

For data replicability and reliability, all diffusion data were first processed by fully automated pipelines using DTIPrep (Liu et al. 2010) followed by TRACULA (Yendiki et al. 2011). Quality control was ensured by DTIPrep, which includes diffusion information check, slice-wise, interlace-wise, and gradient-wise intensity as well as motion check, head motion, and Eddy current artifact correction. All data passed quality checks for further processing.

We implemented TRACULA as a method of automated reconstruction of major WM pathways based on the global probabilistic approach (Jbabdi et al. 2007). TRACULA utilizes prior anatomical information of pathways from a set of training subjects and computes the probability of the WM pathway given the DWI data. Anatomical segmentation labels used by TRACULA were obtained by processing T1-weighted images of participants with the automated cortical parcellation and subcortical segmentation tools in FreeSurfer (Fischl et al. 2002, 2004). All images in each DWI series were aligned to the first nondiffusion-weighted image using affine registration (Jenkinson and Smith

Table 1 Participant demographic and clinical information

	At-Risk (N = 20)	Control (N = 20)	Independent-samples *t*-test *P* value
Age	11.1 ± 1.57	10.65 ± 2.12	0.44
Gender	10 F, 10 M	10 F, 10 M	
IQ (KBIT)	118.25 ± 10.78	111.55 ± 12.64	0.09
Parent lifetime depression	Mother affected: 9	0	
	Father affected: 8	0	
	Both parents affected: 3	0	
CBCL total problems	46.45 ± 10.10	39.40 ± 9.81	0.03*
CBCL internalizing problem score	48.60 ± 9.91	43.20 ± 7.69	0.06
CBCL externalizing problem score	45.45 ± 10.21	43.05 ± 8.91	0.43
CBCL affective problem score	52.70 ± 3.74	51.55 ± 3.76	0.34
CBCL anxiety problem score	53.70 ± 4.76	51.55 ± 3.43	0.11
CDI total *t* score	44.00 ± 5.08	42.42 ± 5.98	0.37

Note: Mean ± SD where appropriate. * Significant result.
F, female; M, male; CBCL, Child Behavior Checklist; CDI, Child Depression Inventory.

2001) and the corresponding diffusion-weighting gradient vectors were reoriented accordingly (Rohde et al. 2004; Leemans and Jones 2009); this commonly used procedure reduces misalignment between images due to head motion and eddy currents. FA images were created by fitting a tensor model to the raw diffusion data using FMRIB's diffusion toolbox (FDT), and then brain-extracted using brain extraction tool (Smith 2002).

Imaging Analyses

The TRACULA pre-processed data were then examined using TBSS (Smith et al. 2004, 2006) for voxel-wise statistical testing throughout the whole brain to localize brain differences between the groups. Individual participants' FA data were aligned to a common space through nonlinear registration. The target image (FMRIB58_FA in standard space) was used for direct template registration for each subject for replicable results. The mean FA image was generated and thinned to create an—alignment-invariant tract representation—the "mean FA skeleton" that represents the centers of all tracts common to the group. Each participant's aligned FA data was then projected onto the FA skeleton. The resulting data (FA on the skeleton-space) were lastly thresholded at 0.2 before being fed into the voxel-wise cross-subject statistical analysis.

Whole-brain voxel-wise analysis on the skeletonized FA maps was first carried out using a general linear model (GLM) to assess group differences and how age interacts with group differently. Randomized nonparametric permutations (number of permutations = 5000) (Winkler et al. 2014) were performed to correct for multiple comparisons across space using the threshold-free cluster enhancement method (Smith and Nichols 2009) and controlling for the family-wise error rate ($P < 0.05$). Main effects of mean differences and slope differences between the groups (the interaction effect between group and age, such as the slope of FA in relation to age) were examined. Individual mean DWI values were averaged across the significant (FA; ROI) voxels in standard space for post hoc examinations (2-way Analysis of variance [ANOVA] and correlation analysis). We also computed the mean MD, RD, and AD values within this ROI to further characterize any WM differences identified by the FA results. The TRACULA-reconstructed major paths for each participant were inspected and overlaid with the individual TBSS significant voxels in the native space to determine which tracts were involved for tract-based assessment.

TRACULA outputted the anisotropy and diffusivity measures averaged over the entire tract for each subject. The assessment on the whole-tract-averaged measures outputted by TRACULA was performed for the identified tracts. In each tract, individually weighted average DWI values were calculated over the pathway distribution corrected for individual variations. Detailed methodology regarding TRACULA-related data processing is provided in Yendiki et al. (2011). The average locations of the paths in standard space (the "spline") were also generated. The spline represented the average location at the center along the cross-sectional volume within the tract and is served to display results of statistical analyses along the tract. To compute statistical testing at the group level, individual values of these DWI measures (FA, RD, MD, and AD) were interpolated from the native space to produce comparable values at corresponding positions along each tract for all subjects. GLM analyses were carried out for tracts identified by TBSS using the FreeSurfer algorithm (mri_glmfit: https://surfer.nmr.mgh.harvard.edu/fswiki/mri_glmfit) to examine the effects from group and age on each DWI measure along each spline point within each tract. P value of 0.05 was used to threshold findings for each spline point statistics. To adjust for multiple comparisons along the spline, clusters >20% proportion of the tract were reported. The significant spline points were displayed on the average tract spline representation. Note that the spline paths served to visualize the statistical results along the tract and did not represent the actual locations where the tract-based assessments were performed.

To examine how the observed significant DWI findings (e.g., in FA) related to clinical measures, voxelwise regressions were applied in the above-defined ROI within-group and across groups to identify linear relationships between DWI values and each clinical measure (CDI and CBCL) while holding the effect of age constant.

To visualize the WM pathways associated with any TBSS-identified ROI, probabilistic tractography was performed, using the ROI as the tractography seed. We used the FMRIB software library (FSL) tractography toolbox (FDT) for automated probabilistic reconstruction of major WM pathways from individual DWIs in native space. This method repetitively samples from the distributions on voxel-wise principal diffusion directions and computes a streamline through these local samples to generate a probabilistic streamline (sample) from the distribution on the location of the true streamline. The local diffusion directions were calculated using the BEDPOSTX toolbox that allowed modeling multiple fiber orientations per voxel. For details about probabilistic tractography implemented by FDT, see Behrens et al. (2003). The output images of individual connectivity paths were normalized by individual total counts of established samples (waytotal), dividing each voxel value by the waytotal number (correcting for individual variations). The individual path images were then nonlinearly registered to the standard space.

Four motion measures were derived by TRACULA and evaluated (Yendiki et al. 2013). 1) Average volume-by-volume translation: this measure was computed by using the translation component of the affine registration from each volume to the first volume to compute the translation vector between each pair of consecutive volumes, and by averaging the magnitudes of these translation vectors over all volumes in each scan. 2) Average volume-by-volume rotation: this measure was derived by using the rotation component of the affine registration from each volume to the first volume to compute the rotation angles between each pair of consecutive volumes, and by averaging the sum of the absolute values of these rotation angles over all volumes in each scan. 3) Percentage of slices with signal drop-out: signal drop-out scores were calculated for each slice in each volume (Benner et al. 2011). Slices with scores larger than 1 were considered likely to have signal drop-out and were thus excluded from the analyses for this study. We then computed the percentage of slices within each scan that had a score >1. 4) Signal drop-out severity: we also computed the average signal drop-out score over all slices in each scan that had a score >1 (Benner et al. 2011).

Results

Quality Assurance: Head Motion

The assessment of head motion measures indicated that motion was unlikely to explain any of the DWI findings. ANOVAs on translation and rotation scores did not yield significant effects of group, age, or a group by age interaction ($Ps > 0.48$). Across all participants and within each group,

there were no significant correlations between the translation score and age (Supplementary Figure 1A) or between the rotation score and age (Supplementary Figure 1B; *Ps* > 0.58, Pearson's correlations). There were no significant correlations between any of the motion measures and any behavioral measure (CBCL and CDI) either within-group or across groups (*Ps* > 0.25, Pearson's correlations). All participants' translation scores were below 2 mm and the rotation scores below 0.2°. Normal percentage of slices with signal drop-out (value = 0%) and average signal drop-out severity score (value = 1) were obtained across all participants. Details regarding head motion measurements and figures are reported in the Supplementary material.

TBSS Whole-Brain Statistics

There were no significant differences between groups on mean FA (At-Risk group = 0.66 ± 0.03; Control group = 0.65 ± 0.04) or on any other DWI measure, with or without controlling for age as the covariate. There was, however, a significant group by age interaction for FA found in the anterior frontal-limbic WM region including the anterior cingulum and the genu of the

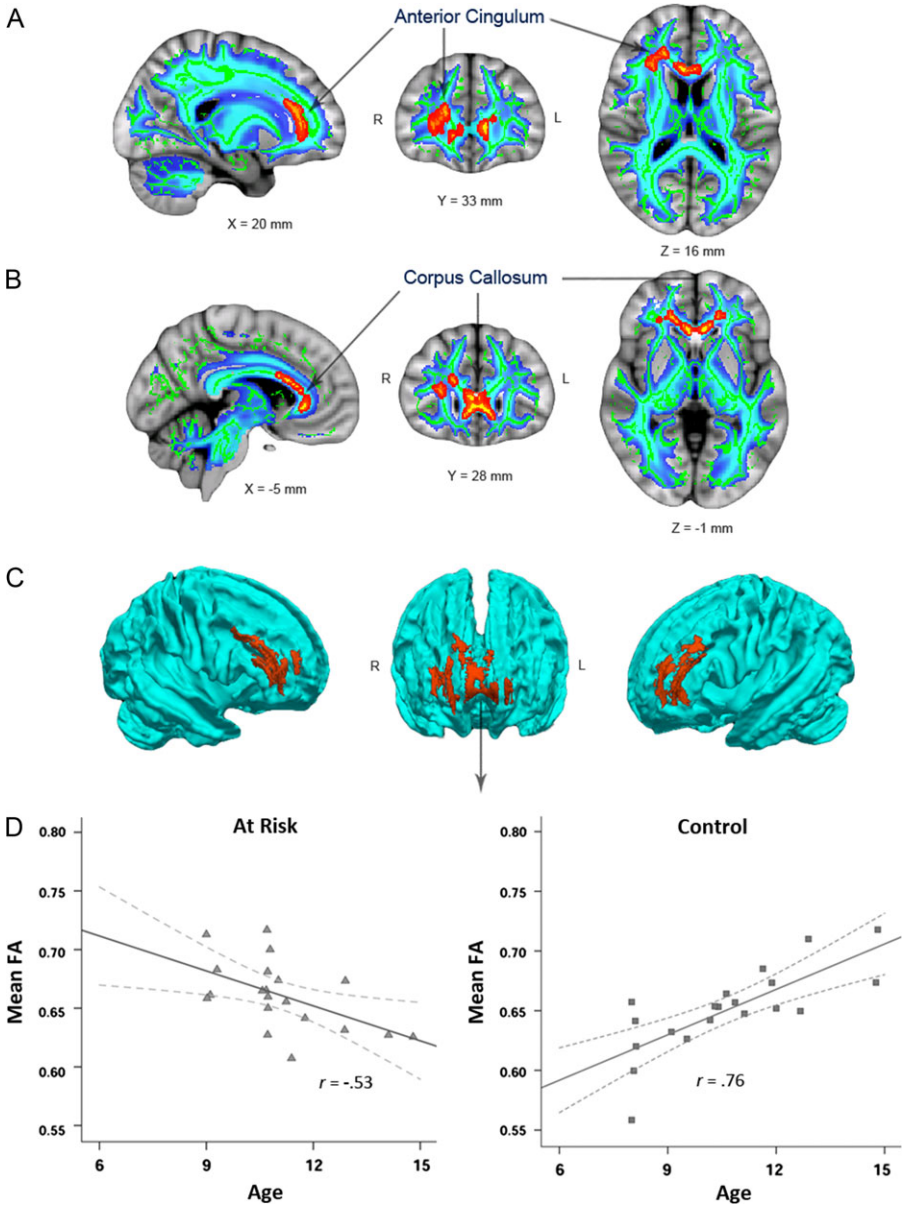

Figure 1. FA in the anterior frontal-limbic WM regions (in red) showed a significant interaction of age by group, with lower FA age-related slope in the At-Risk children in contrast to the Control children. (*A*) The peak significant cluster was observed in the anterior cingulum region, including the anterior limb to the internal capsule (right lateralized). (*B*) The second peak cluster was located in the genu of the corpus callosum, which extended forward into anterior prefrontal regions. Significant voxels were filled out from the skeleton into the mean FA space to visualize the representative local tract regions based on group mean FA. Images were overlaid on the mean FA skeleton of all participants (in green) and the group mean FA (in blue) (thresholded at 0.2 for both image layers). The bottom layer was MNI 152 1-mm standard brain template. (*C*) The 3D images of all significant FA areas (in red) were superimposed on the group mean FA (in blue) (thresholded at 0.2 for both layers). (*D*) Individual mean FA values are plotted (*Y*-axis) in relation to age (*X*-axis) for children in the At-Risk group (left panel) and the Control group (right panel). The At-Risk group showed a significant negative correlation between FA and age, whereas the Control group showed the typical and significant positive correlation between FA and age. Trend prediction was shown in solid lines, with 95% confidence intervals shown in dashed lines.

corpus callosum (Fig. 1; $P < 0.05$, corrected; also see Supplementary Table 1). Post hoc examinations on the mean FA averaged across significant voxels showed that the Control group exhibited a significantly positive correlation between FA and age (Fig. 1D; $r = 0.76$, $P < 0.05$, Pearson's correlation); in contrast, the At-Risk group exhibited a significantly negative correlation between FA and age ($r = -0.53$, $P < 0.05$, Pearson's correlation).

In order to visualize the direction of the age-related differences, we examined in a 2-way ANOVA the effects of group and age on the mean FA extracted across TBSS significant regions. Each group was equally divided into younger (ages 8–11, $N = 10$) and older (ages 11–14, $N = 10$) subgroups. There was a significant interaction between age and mean FA of the TBSS-significant region (Fig. 2) [F (1, 36) = 14.69, $P < 0.001$, 2-way ANOVA]. All results remained significant after controlling for clinical behavioral measures (CBCL and CDI scores). Post hoc comparisons showed that mean FA for the younger children was higher in the At-Risk group ($M = 0.67$, SD = 0.027) than in the Control group ($M = 0.63$, SD = 0.030), whereas mean FA for the older children was lower in the At-Risk group ($M = 0.65$, SD = 0.028) than that in the Control group ($M = 0.67$, SD = 0.025).

As a post hoc behavioral examination for the observed brain results, we compared the At-Risk versus Control behavioral differences for the younger and the older subgroups separately. Only the older At-Risk children exhibited significantly elevated CDI scores than the age-matched older Control children [$t(18) = 2.17$, $P < 0.05$]; independent-samples t-test; there was no significant difference in CDI between the 2 younger subgroups of children. Conversely, only the younger At-Risk children exhibited significantly elevated CBCL total problem scores [$t(18) = 2.84$, $P < 0.05$] and internalizing problem scores [$t(18) = 2.19$, $P < 0.05$]; there were no significant differences in CBCL between the older subgroups of children (Supplementary Table 2).

To supplement the significant FA findings, we further examined the mean MD, RD, and AD values in the ROI that showed the significant interaction in FA. The Control group showed a significant negative correlation between RD and age (Fig. 3A; $r = -0.72$, $P < 0.05$, Pearson's correlations), whereas the At-Risk group showed a significant positive correlation between RD and age ($r = 0.52$, $P < 0.05$, Pearson's correlations). The Control group showed a significant negative correlation between MD and age (Fig. 3B; $r = -56$, $P < 0.05$, Pearson's correlations), whereas the At-Risk group did not show any significant age-correlated change. There was no significant relation between AD and age in either group.

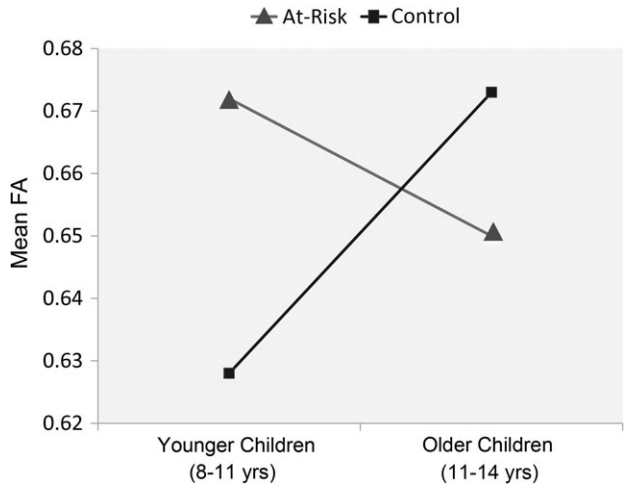

Figure 2. Significant group by age interaction on mean FA averaged across TBSS significant region. Two-way ANOVA (group by age) on the mean FA yielded no main effects of group or age, but a significant group by age interaction. This interaction illustrates the developmental differences found between groups in voxel-level (TBSS).

Brain-Behavioral Correlations with CDI

To assess whether the abnormal FA cross-sectional development observed between the 2 groups was related to symptoms of depression as measured by the CDI scale, we examined the relationship between the FA from the TBSS ROI and the CDI total scores within each group. In the At-Risk group, there was a significant negative correlation between FA and the CDI total scores, located in the dorsal anterior cingulum (dAC) (Fig. 4A; $P < 0.05$, corrected); this correlation remained significant after controlling for age. There was no significant correlation between FA and CDI scores in the ROI for the Control group. There were no significant correlations between the other DWI measures and CDI scores in either group. The individual FA values extracted across the identified dAC cluster demonstrate the negative relationship between FA and CDI in the At-Risk group but not in the Control group (Fig. 4B; $r = -0.57$, $P < 0.05$, Pearson's correlations). Neither group exhibited a significant correlation between FA and CBCL scores.

Tract-Based Assessment

Inspections of individual TRACULA-reconstructed major paths that overlapped with the TBSS-identified region exhibiting a group by age interaction suggested that 3 frontal-limbic tracts were involved, including the anterior forceps (also known as forceps minor), right anterior thalamic radiation (ATR), and the right uncinate (UNC); (Supplementary Figure 2; also shown in Fig. 5A). The tract-based assessment along these 3 frontal-limbic tracts of interest (Fig. 5B) revealed a significant group × age interaction on MD in the anterior forceps (Fig. 5C; $P < 0.05$, corrected for cluster size). Post hoc within-group examinations showed that while the Control group demonstrated an age-related MD decline (Fig. 5D; $r = -0.68$, $P < 0.05$, Pearson's correlations), the At-Risk group did not show any significant MD changes with age. This result is consistent with the TBSS finding in the MD of the frontal-limbic regions. No other significant correlations were observed related to other DWI or the behavioral measures on along these tracts of interest. The whole-tract-averaged assessment on the DWI measures did not show any significant difference between group or any group × age interactions in any of the 3 major tracts (anterior forceps, bilateral UNC, and bilateral ATR) identified as passing through the TBSS voxelwise finding that showed a group × age interaction. Thus, the developmental differences reflect regional specificity that did not extend measurably throughout any of the whole tracts.

Tract Reconstructions

Probabilistic tractography successfully reconstructed the WM pathways connected with the TBSS-identified ROI (Fig. 6), visualizing primarily anterior frontal-limbic tracts including the anterior extensions of the corpus callosum (including the anterior forceps), the right uncinate tract, and the right ATR.

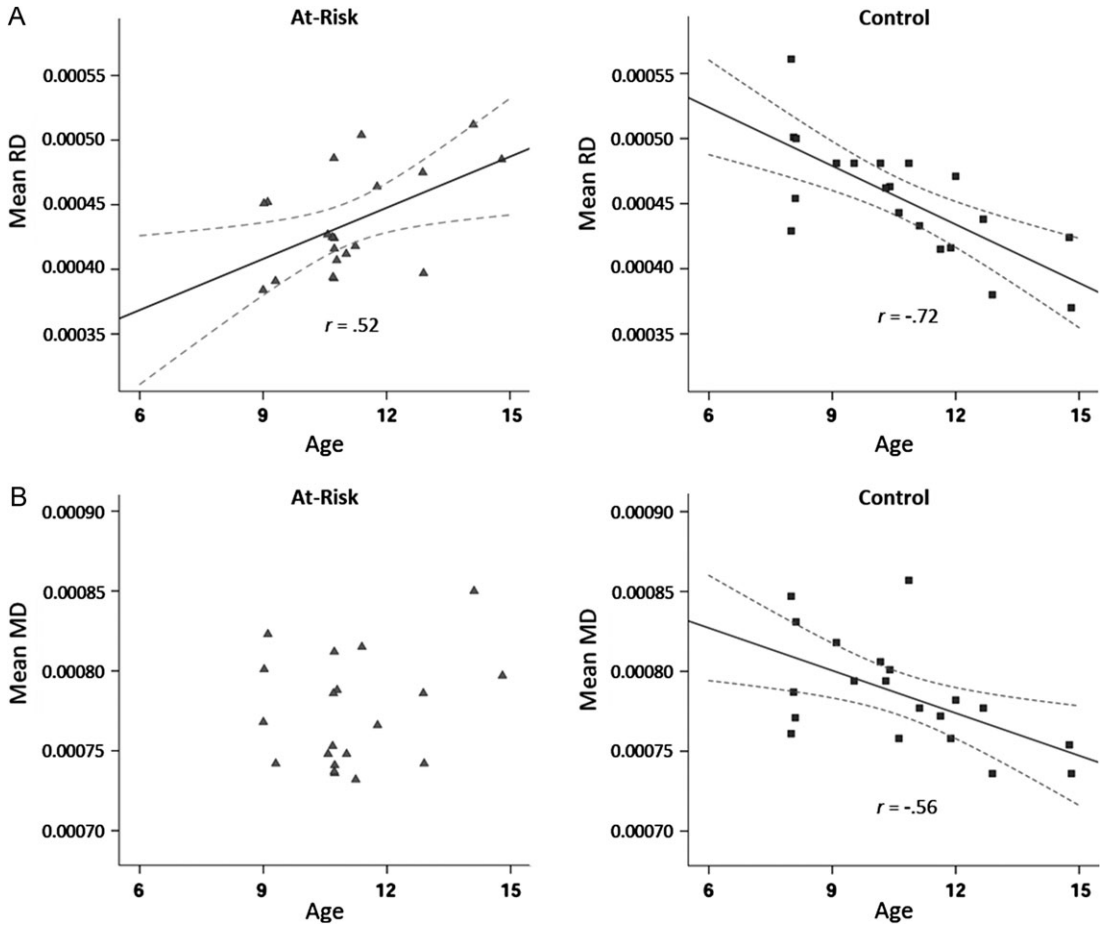

Figure 3. Other diffusivity measures (RD, MD) showed differences in age-related developmental trajectories between groups in the area of where group by age interaction was observed for FA. (*A*) The At-Risk group showed significant and atypical cross-sectional increases of RD with age, whereas the Control group showed significant and typical cross-sectional decreases of RD with age. (*B*) The Control group showed significant and typical cross-sectional decreases of MD with age, whereas the At-Risk group did not show any age-related changes in MD.

Discussion

This study revealed atypical cross-sectional development of fronto-limbic WM pathways associated with familial risk for depression. Non-disordered children with familial risk for MDD, compared with children without such risk, exhibited abnormal WM microstructure maturational patterns in the anterior frontal-limbic tracts. The At-Risk children exhibited atypical age-related decreases of FA in these pathways, in marked contrast to the typical age-related increases of FA exhibited by the Control children without familial risk. Within this frontal-limbic WM ROI, lower FA was associated with-worse scores on a clinical measure of symptoms of depression (elevated CDI scores) for the At-Risk children. To the best of our knowledge, this is the first report of a "developmental" WM brain difference in children at familial risk for MDD.

The 2 groups of children were well matched and did not differ significantly on age, IQ, or gender distribution. Although the At-Risk children had more impaired CBCL scores (primarily driven by the younger subgroup) and the older At-Risk children had more depressive symptoms, all CBCL and CDI scores were below any clinical cutoff in both risk groups. Yet, despite the absence of different diagnoses between the groups, there were distinct age-related differences in WM characteristics between At-Risk and Control groups.

Although no At-Risk child had depression, there were indications that neurodevelopmental differences may have been salient related to increased risk for depression as the At-Risk children approached the adolescent ages when onset of MDD becomes more likely. Only the older At-Risk children had higher depression symptoms (CDI scores) than their age-matched Control children, and only the older At-Risk children had reduced FA relative to their age-matched Control children. Reduced FA has been a consistent finding in pediatric and adult MDD (Drevets et al. 2008; Zhang et al. 2012; de Kwaasteniet et al. 2013; LeWinn et al. 2014).

Impaired Maturation in Anterior Fronto-Limbic White-Matter Pathways

In typical development during childhood and adolescence, FA increases with age and RD and MD decrease with age in the majority of WM tracts (Giorgio et al. 2008; Lebel et al. 2012; Mwangi et al. 2013), reaching maturation at the beginning of adulthood in cross-sectional studies. The Control children in this study exhibited a typical profile of age-related increases of FA and decreases of RD and MD in fronto-limbic WM from childhood to mid-adolescence, which conforms to data reported from 453 healthy participants across ages 5–83 years (Lebel et al. 2012). In sharp contrast, the At-Risk children

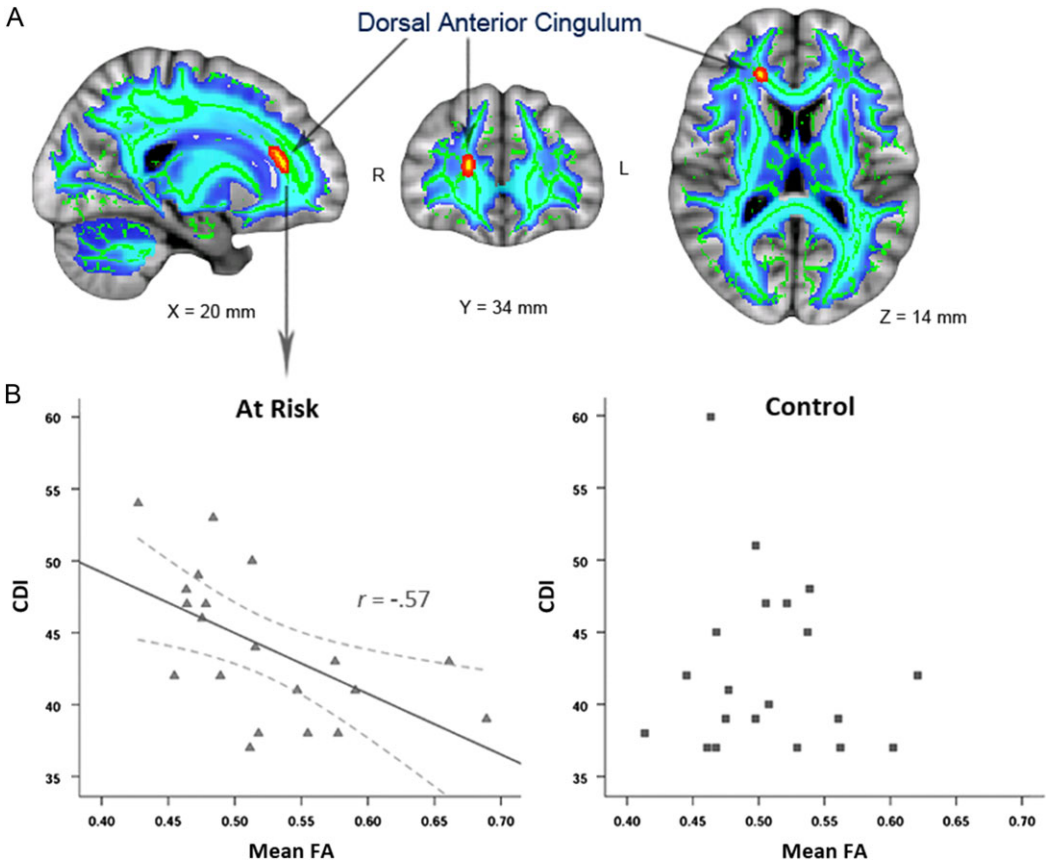

Figure 4. Significant linear relationship between FA and depressive symptoms identified in the anterior cingulum in the At-Risk group. (A) Significant negative correlation between FA and the CDI total score was found in the At-Risk group localized in the dAC region, whereas in the Control group no correlation was found. (B) Individual mean FA values extracted from the identified dAC cluster demonstrated the negative correlation between FA and CDI in the At-Risk group but not in the Control group.

exhibited atypical age-related decreases of FA and increases of RD, and failed to show normal decreases of MD with age in anterior fronto-limbic WM.

FA, the most commonly reported diffusion measure, indicates how variable the diffusion is among different directions (parallel and perpendicular) in a voxel along the local WM pathways. AD measures the strength of diffusion parallel to a tract, RD measures the strength of diffusion perpendicular to a tract, and MD measures the average strength of diffusion in all directions (Pierpaoli and Basser 1996). There has been evidence suggesting that AD is more sensitive to changes in axon fibers, whereas RD is more sensitive to changes in myelin (Song et al. 2002, 2005; Wheeler-Kingshott and Cercignani 2009). It was also suggested that decreases in FA coupled with increases in RD may reflect problems related to myelination (Song et al. 2002). In this study, the difference in maturation that occurred between groups in FA and RD (with a preserved AD) showed that there may be a deficient development related to myelination within the frontal-limbic pathways that is associated with increased risk for mood disorders.

The present findings of abnormal cross-sectional WM development in children with familial risk for MDD parallel previous findings of abnormal gray matter development, as measured by cortical thickness, in a cross-sectional study of adolescent daughters of mothers with recurrent MDD (Foland-Ross et al. 2015). Specifically, there was an interaction between group (at-risk vs. control) and age for thickness in the anterior cingulate cortex (ACC) and anterior insula region. Whereas girls in the control group exhibited the typical negative relationship between age and thickness (i.e., cortical thinning with age), girls in the familial risk group exhibited the reverse pattern. Furthermore, thinner gray matter in the ACC of familial-risk girls was associated with greater difficulty in managing sadness (using scores on the Children's Sadness Management Scale) (Foland-Ross et al. 2015). Accordingly, the current and prior studies provide consistent evidence in children with familial MDD regarding an age-related atypical reversal of both WM and gray-matter ACC maturation, which was related to changes in symptoms of depression (CDI scores) or abilities of mood regulation.

Functional Neuroanatomy of the Fronto-limbic Network

Age-related differences were observed in WM pathways connecting frontal and limbic regions that are often involved in emotion and its regulation (Ochsner and Gross 2005; Buhle et al. 2014), primarily including the anterior cingulum and corpus callosum, as well as the ATR and anterior limb of uncinate tract. The genu and anterior cingulum, both receive axonal input from the ACC (Catani et al. 2002), a brain region known to regulate cognitive and emotional processes (e.g., Bush et al. 2000) and related to psychotherapy outcome for MDD (Carl et al. 2016). The anterior extensions of the genu and anterior cingulate bundles constitute the anterior

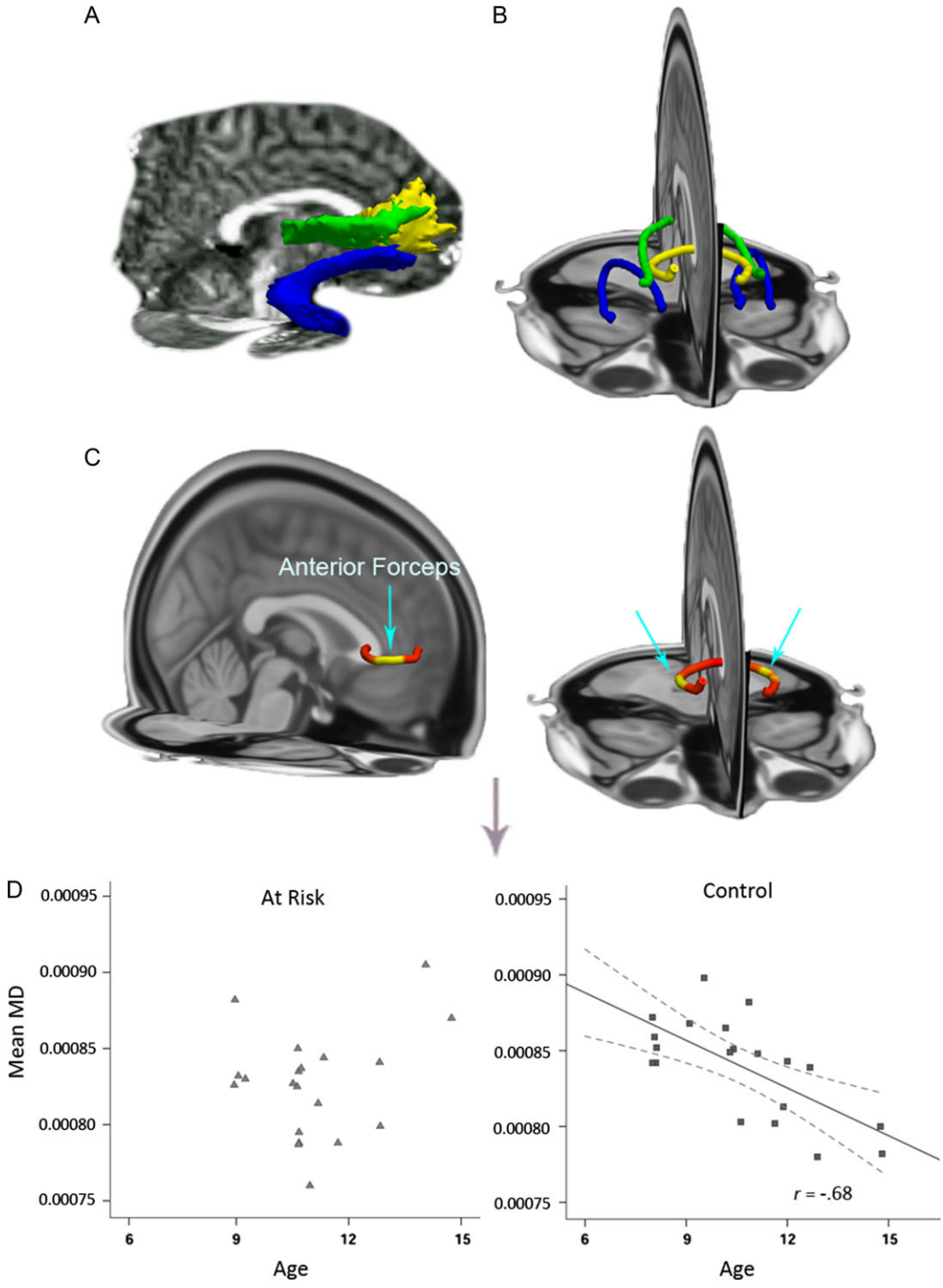

Figure 5. Tract-based assessments revealed the abnormal anterior frontal-limbic tract in the At-Risk children. (*A*) The TRACULA-reconstructed major tracts of interest including the anterior forceps (yellow paths), ATR (ATR; green paths), and uncinate fasciculus (UNC; blue paths) in a 10-year-old At-Risk participant in the native space. (*B*) The group-averaged path representations (splines) of the 3 tracts. (*C*) Regions exhibiting significant age by group differences in the anterior forceps shown on the spline (in yellow). Spline image threshold $P = 0.05$; 20% proportion of the tract was reported adjusting for multiple comparisons. Bottom layer was the MNI 152 1-mm standard brain. (*D*) Mean MD values extracted across all significant spline points were plotted against age for each group. The Control group demonstrated the typical decline of MD with age, whereas the At-Risk group did not show any significant age-related differences in MD.

forceps, which was the only tract that was significantly different cross-sectionally and bilaterally between groups by the MD measure. The anterior forceps connects to lateral and anterior surfaces of prefrontal cortex (PFC) (Catani et al. 2002; Jones et al. 2013), areas that are important for high-level mental operations such as cognitive control and decision making (Christoff and Gabrieli 2000; Owen et al. 2005). Both the PFC and ACC show increased activation with increased cognitive load, as more information must be kept in mind (in working memory) (Arsalidou et al. 2013) or distracting and

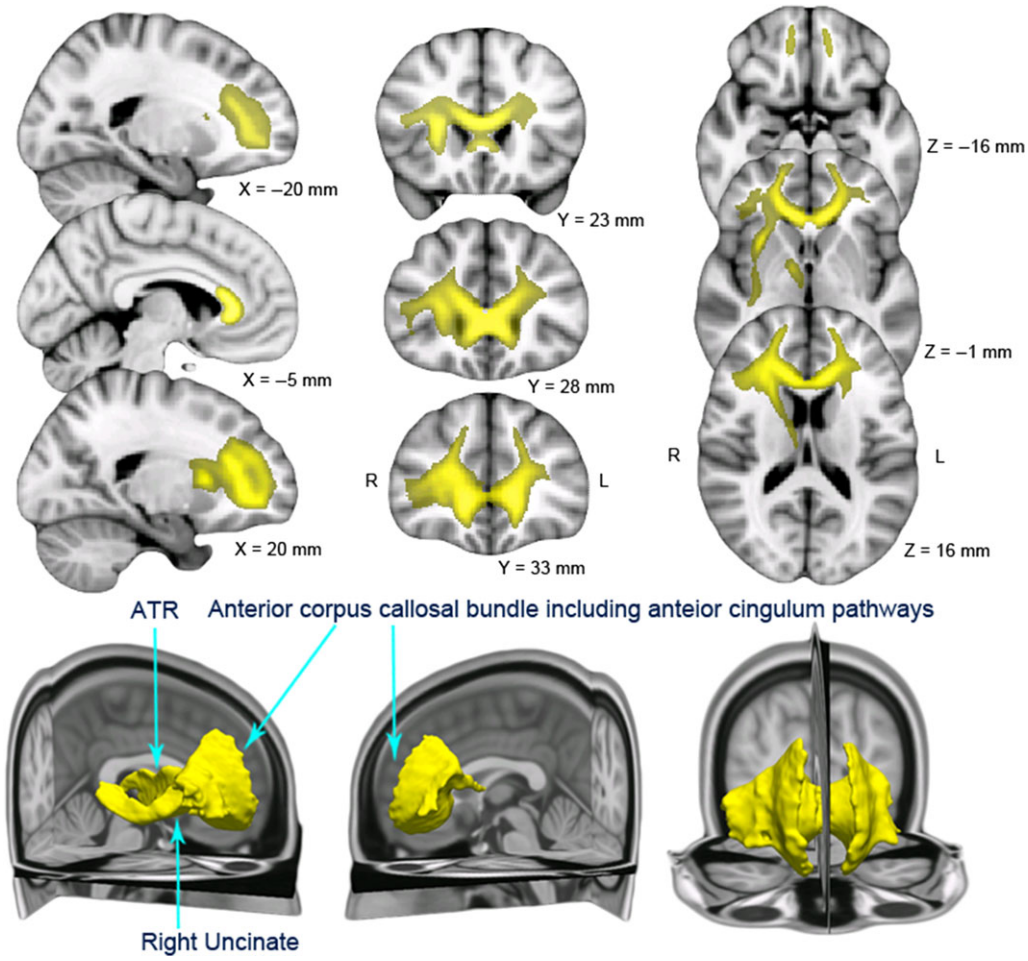

Figure 6. Probabilistic tractography reconstructed the mean connectivity distribution of the frontal-limbic pathways across groups from the TBSS identified ROI. Involved tracts included the anterior corpus callosal bundle, which included the anterior forceps, the right uncinate (anterior limb), and the right ATR. Images were thresholded by a minimum of 5% of the maximum proportion of total streamline connectivity. Bottom layer was the MNI 152 1-mm standard brain.

competing information must be managed (cognitive inhibition) (Rottschy et al. 2012).

The location of impaired WM development in the nondisordered At-Risk children is similar to the locations of abnormality reported in studies of patients with MDD. Reduced FA in these locations was found in adults (de Kwaasteniet et al. 2013; Xu et al. 2013) and adolescents (e.g., LeWinn et al. 2014) with MDD. Lower FA has been reported in bilateral cingulum bundles and subgenual cingulate in adult females without depression but with family history of depression (Keedwell et al. 2012). Furthermore, microstructural alterations in prefrontal WM regions have been identified in the early course of MDD (Li et al. 2007). Abnormalities of the anterior forceps have also been found related to depressive symptoms in adults with brain injury (Strain et al. 2013; Gobbi et al. 2014).

Within all the observed WM regions in which development differentiated the At-Risk children, lower FA in the dorsal subdivision of the anterior cingulate cortex (dACC), correlated with more depressive symptoms (total CDI scores) in the At-Risk children. Although dACC has been associated with cognitive control (e.g., Bush et al. 2000; Botvinick et al. 2001), there is evidence that this region may integrate cognitive and emotional processes via its function in attention and inhibition to emotionally salient information (Phan et al. 2002; Phillips et al. 2003; Etkin et al. 2011; Shackman et al. 2011). Consequently, the dACC has been found to be involved in cognitive control and regulation of negative affect (Giuliani et al. 2011). The current finding of FA in the dorsal ACC circuit being inversely associated with number of depressive symptoms in At-Risk children is consistent with functional imaging on at-risk teenage girls with parental depression who exhibited reduced activation in dorsal ACC and dorsolateral PFC regions during automatic mood regulation (Joormann et al. 2012).

The ATR was found to exhibit atypical cross-sectional maturation in the At-Risk children. The ATR runs in the anterior limb of the internal capsule, connecting the PFC to deep brain structures (Wakana et al., 2004; Coenen et al. 2012) including the thalamus and the nucleus accumbens, brain structures that have been implicated in atypical motivational processes in MDD (Pizzagalli et al. 2009; Carl et al. 2016). The ATR has been suggested as a potential target for lesions or deep brain stimulation in the treatment of affective disorders because of its direct connection between the forebrain and thalamus and the nucleus accumbens (Coenen et al. 2011, 2012; Cho et al. 2015). Gray matter volume of the thalamus in adolescents with MDD appears to have an atypical developmental trajectory, with typical adolescents exhibiting increased volume with age, whereas adolescents with MDD exhibiting decreased volume with age; thalamus volume was also found to significantly correlate with depressive symptoms (Hagan et al. 2015). The current data

provide new structural connectivity evidence suggesting that the ATR may be involved in risk for depression.

The WM differences tended to be right-lateralized, especially in the right uncinate and right ATR, pathways connecting PFC with the limbic systems. The uncinate links limbic structures (e.g., amygdala) with the PFC, connecting brain regions engaged in detecting the emotional significance of information and producing a reaction to it (Catani et al. 2002; Phillips et al. 2003; Kier et al. 2004; Drevets et al. 2008; Von Der Heide et al. 2013), has been associated with mood-related disorders (e.g., Zhang et al. 2012). Adult MDD has often been associated with right-lateralized abnormalities (Shenal et al. 2003). There is evidence that reduced WM FA occurs in right-lateralized pathways connecting the ACC and the amygdala in adolescents with MDD (Cullen et al. 2010). This right lateralization in response to emotional stimuli, however, may develop with age in children (Hung et al. 2012), and may need to be understood in the context of the development of limbic and cortical regions (e.g., Thomason et al. 2009).

The right-dominant WM maturational differences between groups may be related to distinctions between right and left hemispheric contribution to emotion processes. Right-lateralized limbic pathway may be specialized for fast and automatic processing of emotions (e.g., in subliminally presented or masked stimuli), whereas left-lateralized pathway may be specialized for sustained, explicit, and elaborate processing of emotions (e.g., while attending to, or experiencing of, the emotions) that is often related to linguistic analysis of the emotional event (Morris et al. 1998, 1999; Funayama et al. 2001; Gläscher and Adolphs 2003; Noesselt et al. 2005; Hardee et al. 2008; Hung et al. 2010) and with cognitive control and reappraisal of negative emotions (Urry et al. 2009; Ochsner et al. 2012; Uchida et al. 2015). Right-lateralized processes have been associated with depression (Davidson and Fox 1988; Davidson 1992, 1995; Shenal et al. 2003; Schore 2005; Miller et al. 2013). Consistent with greater right-lateralized WM maturational differences in this study, right-lateralized response abnormalities in dorsal ACC and the connected PFC regions were observed in at-risk teenage girls with parental depression during automatic mood regulation (Joormann et al. 2012).

Overall, this study revealed that WM pathways exhibited altered cross-sectional developmental trajectories in children at risk for depression in pathways connecting brain limbic and cortical (prefrontal) regions that are important for emotional responses and motivation, as well as regulation of related behavior (Catani et al. 2002; Phillips et al. 2003; Kier et al. 2004; Ochsner and Gross 2005; Drevets et al. 2008; Pizzagalli et al. 2009; Coenen et al. 2012; Von Der Heide et al. 2013; Buhle et al. 2014; Carl et al. 2016). Abnormal limbic-prefrontal function is characteristic of mood and affective disorders (Drevets 1999; Monkul et al. 2012). Abnormal development of limbic-prefrontal structural connectivity, as at-risk children approach the older ages when depression is more likely to manifest, may impede normal development of adaptive affective functioning, leaving the youth vulnerable to mood-related psychopathology.

Limitations

Some limitations of this study may be noted. First, the study had a moderate subject number across ages 8–14; future studies would benefit from including larger groups with wider age ranges to further characterize and compare differences in WM maturation in different developmental stages. Second, the observed developmental differences were based on a cross-sectional study design; more direct evidence will require a longitudinal design in future research to complement this study. Third, while we excluded children with known developmental conditions such as autism and intellectual disability, we did not assess the children for a history of other psychiatric disorders (e.g., anxiety disorders and conduct disorder). Additionally, we did not exclude children born prematurely, and premature births can lead to neurological complications. In addition, because parental MDD confers a spectrum of risk to offspring (Lieb et al. 2002; Hirshfeld-Becker et al. 2012), albeit dominantly depressive disorders, the at-risk children were also at risk for anxiety and behavioral disorders. Parents with MDD also have higher rates of having comorbid anxiety than the general population. Thus, we cannot rule out that the brain differences we found may be related to disorders other than unipolar depression. Lastly, the relative contributions of genetic and environmental factors on WM development cannot be discerned in this study. The interactions between genetic and environmental factors and how they impact on the brain and behavior over time may be of interest for future research.

Conclusion

This study revealed neuroanatomical differences in WM associated with increased risk for depression due to familial depression. The age-related neurodevelopmental differences in WM anatomy between children with versus without familial risk for depression occurred in PFC-ACC-limbic tracts associated with brain regions important for emotion and its regulation. Further understanding of brain characteristics associated with risk for depression, and how those characteristics change with age as children approach the ages when affective disorders are most likely to be diagnosed, may illuminate not only the developmental pathophysiology of depression and anxiety, but identify those children in greatest need of preventive treatment.

Supplementary Material

Supplementary material can be found at: http://www.cercor.oxfordjournals.org/.

Funding

National Institute of Health (R01 HD036317, R01 MH050657 to J.B.), the Tommy Fuss Fund; the Poitras Center for Affective Disorders Research; the MGH Pediatric Psychopharmacology Council Fund; and a fellowship award from the Canadian Institutes of Health Research (to Y.H.) at the Martinos Center at the McGovern Institute for Brain Research, Harvard—MIT (MFE-135509); National Institute of Health (grants to D.H.B. R01 MH636833, R01 MH/CHD076923, and R01 MH47077 [PI: Rosenbaum]). The funding sources had no involvement in study design; in the collection, analysis and interpretation of data; in the writing of the report; or in the decision to submit the article for publication.

Notes

We thank Drs Anastasia Yendiki and Jeanette Mumford for methodology and biostatistics consultation, and Gretchen Reynolds, Daniel O'Young and Jiahe Zhang for help with collecting the imaging data. This study was carried out at the Athinoula A. Martinos Imaging Center at the McGovern Institute for Brain Research at the Massachusetts Institute of

Technology and Massachusetts General Hospital. *Conflict of Interest*: None declared.

References

Achenbach TM, Rescorla LA. 2001. Manual for ASEBA school-age forms & profile. Burlington (VT): University of Vermont Research Center for Children, Youth & Families.

Aghajani M, Veer IM, van Lang ND, Meens PH, van den Bulk BG, Rombouts SA, Vermeiren RR, van der Wee NJ. 2014. Altered white-matter architecture in treatment-naive adolescents with clinical depression. Psychol Med. 44:2287–2298.

Arsalidou M, Pascual-Leone J, Johnson J, Morris D, Taylor MJ. 2013. A balancing act of the brain: activations and deactivations driven by cognitive load. Brain Behav. 3(3):273–285.

Behrens TE, Woolrich MW, Jenkinson M, Johansen-Berg H, Nunes RG, Clare S, Matthews PM, Brady JM, Smith SM. 2003. Characterization and propagation of uncertainty in diffusion-weighted MR imaging. Magn Reson Med. 50(5):1077–1088.

Benner T, van der Kouwe AJ, Sorensen AG. 2011. Diffusion imaging with prospective motion correction and reacquisition. Magn Reson Med. 66(1):154–167.

Botvinick MM, Braver TS, Barch DM, Carter CS, Cohen JD. 2001. Conflict monitoring and cognitive control. Psychol Rev. 108(3):624–652.

Buhle JT, Silvers JA, Wager TD, Lopez R, Onyemekwu C, Kober H, Weber J, Ochsner KN. 2014. Cognitive reappraisal of emotion: a meta-analysis of human neuroimaging studies. Cereb Cortex. 24(11):2981–2990.

Bush G, Luu P, Posner MI. 2000. Cognitive and emotional influences in anterior cingulate cortex. Trends Cogn Sci. 4(6): 215–222.

Carl H, Walsh E, Eisenlohr-Moul T, Minkel J, Crowther A, Moore T, Gibbs D, Petty C, Bizzell J, Dichter GS, et al. 2016. Sustained anterior cingulate cortex activation during reward processing predicts response to psychotherapy in major depressive disorder. J Affect Disord. 203:204–212.

Catani M, Howard RJ, Pajevic S, Jones DK. 2002. Virtual in vivo interactive dissection of white matter fasciculi in the human brain. Neuroimage. 17(1):77–94.

Chai XJ, Hirshfeld-Becker D, Biederman J, Uchida M, Doehrmann O, Leonard J, Salvatore J, Kenworthy T, Brown A, Kagan E, et al. 2015a. Altered intrinsic functional brain architecture in children at familial risk of major depression. Biol Psychiatry. doi:10.1016/j.biopsych.2015.12.003. (Epublication ahead of print).

Chai XJ, Hirshfeld-Becker D, Biederman J, Uchida M, Doehrmann O, Leonard JA, Salvatore J, Kenworthy T, Brown A, Kagan E, et al. 2015b. Functional and structural brain correlates of risk for major depression in children with familial depression. Neuroimage Clin. 8:398–407.

Cho ZH, Law M, Chi JG, Choi SH, Park SY, Kammen A, Park CW, Oh SH, Kim YB. 2015. An anatomic review of thalamolimbic fiber tractography: ultra-high resolution direct visualization of thalamolimbic fibers anterior thalamic radiation, superolateral and inferomedial medial forebrain bundles, and newly identified septum pellucidum tract. World Neurosurg. 83 (1):54–61.e32.

Christoff K, Gabrieli JDE. 2000. The frontopolar cortex and human cognition: evidence for a rostrocaudal hierarchical organization within the human prefrontal cortex. Psychobiology. 28(2):168–186.

Coenen VA, Schlaepfer TE, Maedler B, Panksepp J. 2011. Cross-species affective functions of the medial forebrain bundle: implications for the treatment of affective pain and depression in humans. Neurosci Biobehav Rev. 35: 1971–1981.

Coenen VA, Panksepp J, Hurwitz TA, Urbach H, Madler B. 2012. Human medial forebrain bundle (MFB) and anterior thalamic radiation (ATR): imaging of two major subcortical pathways and the dynamic balance of opposite affects in understanding depression. J Neuropsychiatry Clin Neurosci. 24(2):223–236.

Cullen KR, Klimes-Dougan B, Muetzel R, Mueller BA, Camchong J, Houri A, Kurma S, Lim KO. 2010. Altered white matter microstructure in adolescents with major depression: a preliminary study. J Am Acad Child Adolesc Psychiatry. 49(2): 173–183.e1.

Davidson RJ. 1992. Anterior cerebral asymmetry and the nature of emotion. Brain Cogn. 20(1):125–151.

Davidson R. 1995.Cerebral asymmetry, emotion, and affective style. In: Davidson R, Hugdahl K editors. Brain asymmetry. Cambridge (MA): MIT Press. p. 361–387.

Davidson R, Fox N. 1988. Cerebral asymmetry and emotion: developmental and individual differences. In: Molfese D, Segalowitz S, editors. Brain lateralization in children: developmental considerations. New York (NY): Guilford Press. p. 191–206.

de Kwaasteniet B, Ruhe E, Caan M, Rive M, Olabarriaga S, Groefsema M, Heesink L, van Wingen G, Denys D. 2013. Relation between structural and functional connectivity in major depressive disorder. Biol Psychiatry. 74(1):40–47.

Drevets WC. 1999. Prefrontal cortical-amygdalar metabolism in major depression. Ann NY Acad Sci. 877:614–637.

Drevets WC, Price JL, Simpson JR Jr, Todd RD, Reich T, Vannier M, Raichle ME. 1997. Subgenual prefrontal cortex abnormalities in mood disorders. Nature. 386(6627):824–827.

Drevets WC, Price JL, Furey ML. 2008. Brain structural and functional abnormalities in mood disorders: implications for neurocircuitry models of depression. Brain Struct Funct. 213(1–2):93–118.

Etkin A, Egner T, Kalisch R. 2011. Emotional processing in anterior cingulate and medial prefrontal cortex. Trends Cogn Sci. 15(2):85–93.

First MB, Spitzer RL, Gibbon M, Williams JBW. 1995. Structured clinical interview for DSM-IV axis I disorders (clinician version). New York (NY): New York State Psychiatric Institute Biometrics Department.

Fischl B, Salat DH, Busa E, Albert M, Dieterich M, Haselgrove C, van der Kouwe A, Killiany R, Kennedy D, Klaveness S, et al. 2002. Whole brain segmentation: automated labeling of neuroanatomical structures in the human brain. Neuron. 33 (3):341–355.

Fischl B, Salat DH, van der Kouwe AJ, Makris N, Segonne F, Quinn BT, Dale AM. 2004. Sequence-independent segmentation of magnetic resonance images. Neuroimage. 23 (Suppl. 1):S69–S84.

Foland-Ross LC, Gilbert BL, Joormann J, Gotlib IH. 2015. Neural markers of familial risk for depression: an investigation of cortical thickness abnormalities in healthy adolescent daughters of mothers with recurrent depression. J Abnorm Psychol. 124(3):476–485.

Funayama ES, Grillon C, Davis M, Phelps EA. 2001. A double dissociation in the affective modulation of startle in humans: effects of unilateral temporal lobectomy. J Cogn Neurosci. 13 (6):721–729.

Giorgio A, Watkins KE, Douaud G, James AC, James S, De Stefano N, Matthews PM, Smith SM, Johansen-Berg H. 2008. Changes in white matter microstructure during adolescence. Neuroimage. 39(1):52–61.

Giuliani NR, Drabant EM, Gross JJ. 2011. Anterior cingulate cortex volume and emotion regulation: is bigger better? Biol Psychol. 86(3):379–382.

Gläscher J, Adolphs R. 2003. Processing of the arousal of subliminal and supraliminal emotional stimuli by the human amygdala. J Neurosci. 23(32):10274–10282.

Gobbi C, Rocca MA, Pagani E, Riccitelli GC, Pravata E, Radaelli M, Martinelli-Boneschi F, Falini A, Copetti M, Comi G, et al. 2014. Forceps minor damage and co-occurrence of depression and fatigue in multiple sclerosis. Mult Scler. 20(12): 1633–1640.

Hagan CC, Graham JME, Tait R, Widmer B, van Nieuwenhuizen AO, Ooi C, Whitaker KJ, Simas T, Bullmore ET, Lennox BR, et al. 2015. Adolescents with current major depressive disorder show dissimilar patterns of age-related differences in ACC and thalamus. NeuroImage Clin. 7:391–399.

Hardee JE, Thompson JC, Puce A. 2008. The left amygdala knows fear: laterality in the amygdala response to fearful eyes. Soc Cogn Affect Neurosci. 3(1):47–54.

Hirshfeld-Becker DR, Micco JA, Henin A, Petty C, Faraone SV, Mazursky H, Bruett L, Rosenbaum JF, Biederman J. 2012. Psychopathology in adolescent offspring of parents with panic disorder, major depression, or both: a 10-year follow-up. Am J Psychiatry. 169(11):1175–1184.

Huang H, Fan X, Williamson DE, Rao U. 2011. White matter changes in healthy adolescents at familial risk for unipolar depression: a diffusion tensor imaging study. Neuropsychopharmacology. 36(3):684–691.

Hung Y, Smith ML, Bayle DJ, Mills T, Cheyne D, Taylor MJ. 2010. Unattended emotional faces elicit early lateralized amygdala–frontal and fusiform activations. Neuroimage. 50(2):727–733.

Hung Y, Smith ML, Taylor MJ. 2012. Development of ACC-amygdala activation in processing unattended fear. Neuroimage. 60(1):545–552.

Jbabdi S, Woolrich MW, Andersson JL, Behrens TE. 2007. A Bayesian framework for global tractography. Neuroimage. 37(1):116–129.

Jenkinson M, Smith S. 2001. A global optimisation method for robust affine registration of brain images. Med Image Anal. 5(2):143–156.

Jones DK, Christiansen KF, Chapman RJ, Aggleton JP. 2013. Distinct subdivisions of the cingulum bundle revealed by diffusion MRI fibre tracking: implications for neuropsychological investigations. Neuropsychologia. 51(1):67–78.

Joormann J, Cooney RE, Henry ML, Gotlib IH. 2012. Neural correlates of automatic mood regulation in girls at high risk for depression. J Abnorm Psychol. 121(1):61–72.

Kaufman AS, Kaufman NL. 2004. Kaufman brief intelligence test. 2nd ed. Bloomington (MN): Pearson Inc.

Keedwell PA, Chapman R, Christiansen K, Richardson H, Evans J, Jones DK. 2012. Cingulum white matter in young women at risk of depression: the effect of family history and anhedonia. Biol Psychiatry. 72(4):296–302.

Kier EL, Staib LH, Davis LM, Bronen RA. 2004. MR imaging of the temporal stem: anatomic dissection tractography of the uncinate fasciculus, inferior occipitofrontal fasciculus, and meyer's loop of the optic radiation. AJNR Am J Neuroradiol. 25(5):677–691.

Korgaonkar MS, Williams LM, Song YJ, Usherwood T, Grieve SM. 2014. Diffusion tensor imaging predictors of treatment outcomes in major depressive disorder. Br J Psychiatry. 205(4):321–328.

Kovacs M. 1985. The Children's Depression Inventory (CDI). Psychopharmacol Bull. 21(4):995–998.

Lebel C, Gee M, Camicioli R, Wieler M, Martin W, Beaulieu C. 2012. Diffusion tensor imaging of white matter tract evolution over the lifespan. Neuroimage. 60(1):340–352.

Leemans A, Jones DK. 2009. The B-matrix must be rotated when correcting for subject motion in DTI data. Magn Reson Med. 61:1336–1349.

LeWinn KZ, Connolly CG, Wu J, Drahos M, Hoeft F, Ho TC, Simmons AN, Yang TT. 2014. White matter correlates of adolescent depression: structural evidence for frontolimbic disconnectivity. J Am Acad Child Adolesc Psychiatry. 53(8): 899,909, 909.e1-7.

Lewinsohn PM, Clarke GN, Seeley JR, Rohde P. 1994. Major depression in community adolescents: age at onset, episode duration, and time to recurrence. J Am Acad Child Adolesc Psychiatry. 33(6):809–818.

Li L, Ma N, Li Z, Tan L, Liu J, Gong G, Shu N, He Z, Jiang T, Xu L. 2007. Prefrontal white matter abnormalities in young adult with major depressive disorder: a diffusion tensor imaging study. Brain Res. 1168:124–128.

Lieb R, Isensee B, Hofler M, Pfister H, Wittchen HU. 2002.Parental major depression and the risk of depression and other mental disorders in offspring: a prospective-longitudinal community study. Arch Gen Psychiatry. 59(4):365–374.

Liu Z, Wang Y, Gerig G, Gouttard S, Tao R, Fletcher T, Styner M. 2010. Quality control of diffusion weighted images. Proc Soc Photo Opt Instrum Eng. doi:7628:10.1117/12.844748.

Luking KR, Repovs G, Belden AC, Gaffrey MS, Botteron KN, Luby JL, Barch DM. 2011. Functional connectivity of the amygdala in early-childhood-onset depression. J Am Acad Child Adolesc Psychiatry. 50(10):1027–1041.e3.

Mannie ZN, Taylor MJ, Harmer CJ, Cowen PJ, Norbury R. 2011. Frontolimbic responses to emotional faces in young people at familial risk of depression. J Affect Disord. 130(1–2): 127–132.

Miller GA, Crocker LD, Spielberg JM, Infantolino ZP, Heller W. 2013. Issues in localization of brain function: the case of lateralized frontal cortex in cognition, emotion, and psychopathology. Front Integr Neurosci. 7:2. doi:10.3389/fnint.2013.00002.

Monk CS, Klein RG, Telzer EH, Schroth EA, Mannuzza S, Moulton JL3rd, Guardino M, Masten CL, McClure-Tone EB, Fromm S, et al. 2008. Amygdala and nucleus accumbens activation to emotional facial expressions in children and adolescents at risk for major depression. Am J Psychiatry. 165(1):90–98.

Monkul ES, Silva LA, Narayana S, Peluso MA, Zamarripa F, Nery FG, Najt P, Li J, Lancaster JL, Fox PT, et al. 2012. Abnormal resting state corticolimbic blood flow in depressed unmedicated patients with major depression: a (15)O-H(2)O PET study. Hum Brain Mapp. 33(2):272–279.

Morris JS, Friston KJ, Büchel C, Frith CD, Young AW, Calder AJ, Dolan RJ. 1998. A neuromodulatory role for the human amygdala in processing emotional facial expressions. Brain. 121(1):47–57.

Morris JS, Ohman A, Dolan RJ. 1999. A subcortical pathway to the right amygdala mediating "unseen" fear. Proc Natl Acad Sci USA. 96(4):1680–1685.

Mwangi B, Hasan KM, Soares JC. 2013. Prediction of individual subject's age across the human lifespan using diffusion tensor imaging: A machine learning approach. Neuroimage. 75: 58–67.

Noesselt T, Driver J, Heinze HJ, Dolan R. 2005. Asymmetrical activation in the human brain during processing of fearful faces. Curr Biol. 15(5):424–429.

Ochsner K, Gross J. 2005. The cognitive control of emotion. Trends Cogn Sci (Regul Ed). 9(5):242–249.

Ochsner KN, Silvers JA, Buhle JT. 2012. Functional imaging studies of emotion regulation: a synthetic review and evolving model of the cognitive control of emotion. Ann NY Acad Sci. 1251:E1–E24.

Ongur D, Drevets WC, Price JL. 1998. Glial reduction in the subgenual prefrontal cortex in mood disorders. Proc Natl Acad Sci USA. 95(22):13290–13295.

Orvaschel H. 1994. Schedule for affective disorder and schizophrenia for school-age children—Epidemiologic version 5th ed. Fort Lauderdale (FL): Nova Southeastern University, Center for Psychological Studies.

Owen AM, McMillan KM, Laird AR, Bullmore E. 2005. N-back working memory paradigm: a meta-analysis of normative functional neuroimaging studies. Hum Brain Mapp. 25(1):46–59.

Phan KL, Wager T, Taylor SF, Liberzon I. 2002. Functional neuroanatomy of emotion: a meta-analysis of emotion activation studies in PET and fMRI. Neuroimage. 16(2):331–348.

Phillips ML, Drevets WC, Rauch SL, Lane R. 2003. Neurobiology of emotion perception I: the neural basis of normal emotion perception. Biol Psychiatry. 54(5):504–514.

Pierpaoli C, Basser PJ. 1996. Toward a quantitative assessment of diffusion anisotropy. Magn Reson Med. 36(6):893–906.

Pizzagalli DA, Holmes AJ, Dillon DG, Goetz EL, Birk JL, Bogdan R, Dougherty DD, Iosifescu DV, Rauch SL, Fava M. 2009. Reduced caudate and nucleus accumbens response to rewards in unmedicated subjects with major depressive disorder. Am J Psychiatry. 166(6):702–710.

Rohde GK, Barnett AS, Basser PJ, Marenco S, Pierpaoli C. 2004. Comprehensive approach for correction of motion and distortion in diffusion-weighted MRI. Magn Reson Med. 51(1): 103–114.

Rottschy C, Langner R, Dogan I, Reetz K, Laird AR, Schulz JB, Fox PT, Eickhoff SB. 2012. Modelling neural correlates of working memory: a coordinate-based meta-analysis. Neuroimage. 60(1):830–846.

Sacher J, Neumann J, Funfstuck T, Soliman A, Villringer A, Schroeter ML. 2012. Mapping the depressed brain: a meta-analysis of structural and functional alterations in major depressive disorder. J Affect Disord. 140(2):142–148.

Schore AN. 2005. Back to basics: Attachment, affect regulation, and the developing right brain: Linking developmental neuroscience to pediatrics. Pediatr Rev. 26(6):204–217.

Shackman AJ, Salomons TV, Slagter HA, Fox AS, Winter JJ, Davidson RJ. 2011. The integration of negative affect, pain and cognitive control in the cingulate cortex. Nat Rev Neurosci. 12(3):154–167.

Shenal BV, Harrison DW, Demaree HA. 2003. The neuropsychology of depression: a literature review and preliminary model. Neuropsychol Rev. 13(1):33–42.

Smith SM. 2002. Fast robust automated brain extraction. Hum Brain Mapp. 17(3):143–155.

Smith SM, Jenkinson M, Woolrich MW, Beckmann CF, Behrens TE, Johansen-Berg H, Bannister PR, De Luca M, Drobnjak I, Flitney DE, et al. 2004. Advances in functional and structural MR image analysis and implementation as FSL. Neuroimage. 23(Suppl. 1):S208–S219.

Smith SM, Jenkinson M, Johansen-Berg H, Rueckert D, Nichols TE, Mackay CE, Watkins KE, Ciccarelli O, Cader MZ, Matthews PM, et al. 2006. Tract-based spatial statistics: voxelwise analysis of multi-subject diffusion data. Neuroimage. 31(4):1487–1505.

Smith SM, Nichols TE. 2009. Threshold-free cluster enhancement: addressing problems of smoothing, threshold dependence and localisation in cluster inference. Neuroimage. 44(1):83–98.

Song SK, Sun SW, Ramsbottom MJ, Chang C, Russell J, Cross AH. 2002. Dysmyelination revealed through MRI as increased radial (but unchanged axial) diffusion of water. Neuroimage. 17(3):1429–1436.

Song SK, Yoshino J, Le TQ, Lin SJ, Sun SW, Cross AH, Armstrong RC. 2005. Demyelination increases radial diffusivity in corpus callosum of mouse brain. Neuroimage. 26(1):132–140.

Strain J, Didehbani N, Cullum CM, Mansinghani S, Conover H, Kraut MA, Hart J Jr, Womack KB. 2013. Depressive symptoms and white matter dysfunction in retired NFL players with concussion history. Neurology. 81(1):25–32.

Stuhrmann A, Suslow T, Dannlowski U. 2011. Facial emotion processing in major depression: a systematic review of neuroimaging findings. Biol Mood Anxiety Disord. 1(1):10.

Thomason ME, Race E, Burrows B, Whitfield-Gabrieli S, Glover GH, Bagrieli JDE. 2009. Development of spatial and verbal working memory capacity in the human brain. J Cogn Neurosci. 21(2):316–332.

Uchida M, Biederman J, Gabrieli JDE, Micco J, de los Angeles C, Brown A, Kenworthy T, Kagan E, Whitfield-Gabrieli S. 2015. Emotion regulation ability varies in relation to intrinsic functional brain architecture. Soc Cogn Affect Neurosci. 10: 1738–1748.

Urry HL, van Reekum CM, Johnstone T, Davidson RJ. 2009. Individual differences in some (but not all) medial prefrontal regions reflect cognitive demand while regulating unpleasant emotion. Neuroimage. 47(3):852–863.

Von Der Heide RJ, Skipper LM, Klobusicky E, Olson IR. 2013. Dissecting the uncinate fasciculus: disorders, controversies and a hypothesis. Brain. 136(Pt 6):1692–1707.

Wakana S, Jiang H, Nagae-Poetscher LM, van Zijl PC, Mori S. 2004. Fiber tract-based atlas of human white matter anatomy. Radiology. 230(1):77–87.

Weissman MM, Wickramaratne P, Nomura Y, Warner V, Pilowsky D, Verdeli H. 2006. Offspring of depressed parents: 20 years later. Am J Psychiatry. 163(6):1001–1008.

Wheeler-Kingshott CA, Cercignani M. 2009. About "axial" and "radial" diffusivities. Magn Reson Med. 61(5):1255–1260.

Williamson DE, Birmaher B, Axelson DA, Ryan ND, Dahl RE. 2004. First episode of depression in children at low and high familial risk for depression. J Am Acad Child Adolesc Psychiatry. 43(3):291–297.

Winkler AM, Ridgway GR, Webster MA, Smith SM, Nichols TE. 2014. Permutation inference for the general linear model. Neuroimage. 92:381–397.

Xu K, Jiang W, Ren L, Ouyang X, Jiang Y, Wu F, Kong L, Womer F, Liu Z, Blumberg HP, et al. 2013. Impaired interhemispheric connectivity in medication-naive patients with major depressive disorder. J Psychiatry Neurosci. 38(1):43–48.

Yendiki A, Panneck P, Srinivasan P, Stevens A, Zollei L, Augustinack J, Wang R, Salat D, Ehrlich S, Behrens T, et al. 2011. Automated probabilistic reconstruction of white-matter pathways in health and disease using an atlas of the underlying anatomy. Front Neuroinform. 5:23.

Yendiki A, Koldewyn K, Kakunoori S, Kanwisher N, Fischl B. 2013. Spurious group differences due to head motion in a diffusion MRI study. Neuroimage. 88C:79–90.

Zhang A, Leow A, Ajilore O, Lamar M, Yang S, Joseph J, Medina J, Zhan L, Kumar A. 2012. Quantitative tract-specific measures of uncinate and cingulum in major depression using diffusion tensor imaging. Neuropsychopharmacology. 37(4): 959–967.